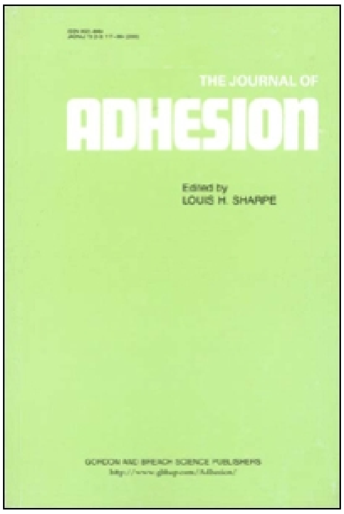

The Journal of Adhesion
Publication details, including instructions for authors and subscription information:
http://www.informaworld.com/smpp/title~content=t713453635

Surface Analysis of Etched and Anodised Aluminium-Copper Alloys

A. Datta[a]; R. A. Pethrick[a]; S. Affrossman[a]
[a] Department of Pure & Applied Chemistry, University of Strathclyde, Glasgow, Scotland

To cite this Article Datta, A. , Pethrick, R. A. and Affrossman, S.(1982) 'Surface Analysis of Etched and Anodised Aluminium-Copper Alloys', The Journal of Adhesion, 15: 1, 13 — 25
To link to this Article: DOI: 10.1080/00218468208073213
URL: http://dx.doi.org/10.1080/00218468208073213

J. Adhesion, 1982, Vol. 15, pp. 13–25
0021-8464/82/1501-0013 $06.50/0

Printed in Great Britain

Surface Analysis of Etched and Anodised Aluminium-Copper Alloys

A. DATTA, R. A. PETHRICK and S. AFFROSSMAN†
Department of Pure & Applied Chemistry, University of Strathclyde, Glasgow G1 1XL, Scotland

(*Received March 29, 1982; in final form May 11, 1982*)

SEM-EDAX studies of etched and anodised aluminium-copper alloys show that there is an excess of copper in the etch pits. The depth profiles of components of the alloys are obtained by XPS-ion etching, and the results are interpreted taking into account the observed lateral inhomogeneous distribution of the elements.

INTRODUCTION

It is known that the chemical composition of an adhered surface can have a major effect on the long term durability of a bonded structure. For instance, it has been shown that in the case of aluminium, the presence of copper and magnesium is detrimental to the environmental durability of the bond. The existence of copper in aluminium has been shown by ion implantation[1] and by Auger electron spectroscopy[2] to hinder the growth of oxide layers on the aluminium. Moreover, it is known that copper can form a $CuAl_2$ precipitate.[3] The combination of cathodic $CuAl_2$ precipitates and the more anodic aluminium matrix constitutes a galvanic couple, which may lead to an electrochemical dissolution of the matrix material in an adverse environment.[4] Since the prevalent method of surface preparation of aluminium adherends involves the process of acid etching followed by anodization, it would be expected that regions of high copper, in copper containing aluminium alloys, would react differently from the rest of the substrate, during the etching and anodization processes. Consequently, the surface topography of a copper

---

† To whom enquiries should be addressed.

containing aluminium alloy would be different from that of a copper free sample. Since one of the mechanisms of adhesive bonding is probably a mechanical interlocking between the adhesive and adherend, any possible variation in the surface structure, after the surface pretreatment procedure, would be expected to have a substantial effect on the overall stability of the adhesive bond.

The complex morphology and chemical composition of the surface are amenable to investigation by modern surface techniques. Because of the variation of structure laterally and perpendicular to the surface, a combination of electron microscopy and depth analysis is advantageous as noted by several authors. Pattnaik and Meakin have applied SEM, RHEED and Auger to treated alloy surfaces,[5] and have shown the pit structures formed on etching. Sun, *et al.*, have used SEM and Auger and have paid particular attention to the effect of ion bombardment on the structure of the small pores in the oxide.[6] They point out the necessity to allow for the effect of surface roughness on depth analysis, and equate the latter to the oxide cell height. Kinloch *et al.*, have used SEM and XPS to examine bonds fractured *in vacuo* and have emphasized the need to correlate surface analysis with fracture studies on carefully designed bonds.[7] In this paper we examine the contribution of the etch pit structure of copper containing alloys to the depth analysis by means of SEM/EDAX and XPS.

EXPERIMENTAL

Three different commercially available aluminium alloys were used in the present study. These samples, referred to hereafter as samples A, B and C, had specified copper contents of 0.1, 2.4, 5.5 (per cent by weight) respectively. The temper treatment of these specimens involved solution heat treatment followed by rapid quenching and subsequent natural aging.

Two stubs (diameter = 0.5 in., thickness = 0.3 in.) of each aluminium alloy were prepared. These stubs were then subjected to a chromic acid etching process.[8] This consisted of first degreasing the samples with trichloroethane followed by washing in an alkaline solution containing 5% sodium carbonate and a detergent. The stubs were then etched at 60–65°C for 30 minutes in a solution containing 150 g/l of sulphuric acid (S.G. = 1.84), 50 g/l of chromic oxide and 50 ppm of copper. The stubs were then washed repeatedly with cold de-ionized water and air dried. One stub of each of the three aluminium alloys was analysed after the etching process. The other stub of each alloy was then anodized in a 10% w/w aqueous solution of phosphoric acid at 15 V for 25 min at 23–25°C according to the Boing specification BAC 5555.[9] The current density was about 15 mA/cm^2. Finally, the stubs were washed with de-ionized water, air-dried and then analyzed.

The surface morphology of the samples was examined with a Phillips PSEM 500 Scanning Electron microscope and the energy dispersive X-ray analysis was carried out on an energy dispersive X-ray analysis (EDAX) unit (Link systems Model 860) coupled with the electron microscope. The analysis was done using an accelerating voltage of 25 kV and with a beam diameter of 0.25 μm.

The XPS spectra were obtained with a Vacuum Science Workshop 65 mm analyser. The angles between the sample and the X-rays, and the sample and analyser were 45°.

Depth profiling was carried out with 6 kV Argon ions at normal incidence to the surface and average current density $\sim 50\ \mu$A cm^{-2}.

RESULTS

Scanning electron microscopy

The distribution of copper over the surface was found to be non uniform in both the copper containing alloys, as received, Figure 1.

A comparison of the electron micrographs of treated samples of A, B and C shows that there is a drastic difference in their surface morphologies, Figures 2–4.

Considering firstly sample A, both the etched and anodized samples show a pitted structure. In the etched specimen the pits are randomly distributed and have an average diameter of around 2 μm. In the anodized sample, in addition to the pits (average diameter = 2 μm) produced during etching, a uniform distribution of much smaller pores is evident.[7] It is known[8] that phosphoric acid anodization of aluminium, under the conditions of the Boeing specification, produces a porous oxide layer around 2000 Å thick, the average diameter of the pores being about 320 Å.

The EDAX studies of both etched and anodized stubs of sample A, show that there is an approximately uniform distribution of aluminium over the surface analysed. Using electrons accelerated under a voltage of 25 KV the depth of penetration into the surface would be around 1 μm. Hence the fact that aluminium is evenly distributed over the surface analysed shows that the pits are all much less than 1 μm deep. No copper could be detected during the analysis.

The etched and anodized specimens of sample B show a surface structure which is markedly different from that of the specimens of sample A. Both the etched and anodized stubs are characterized by pits of varying sizes. The diameter of the pits varies from 2 μm to around 12 μm and these must have

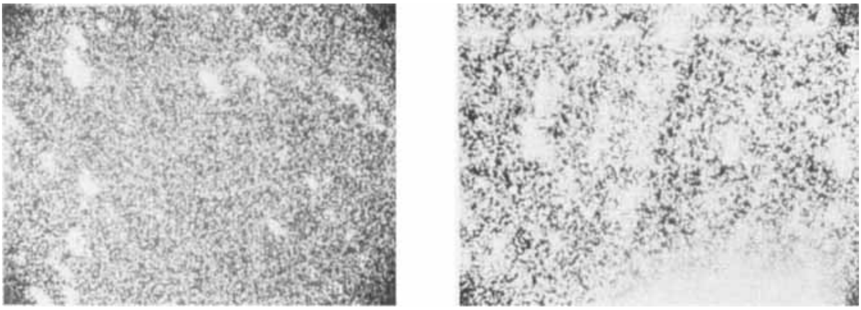

FIGURE 1 Copper distributions on as received alloys. Left, 2.4% Cu sample; right, 5.5% Cu sample. Magnification 2000.

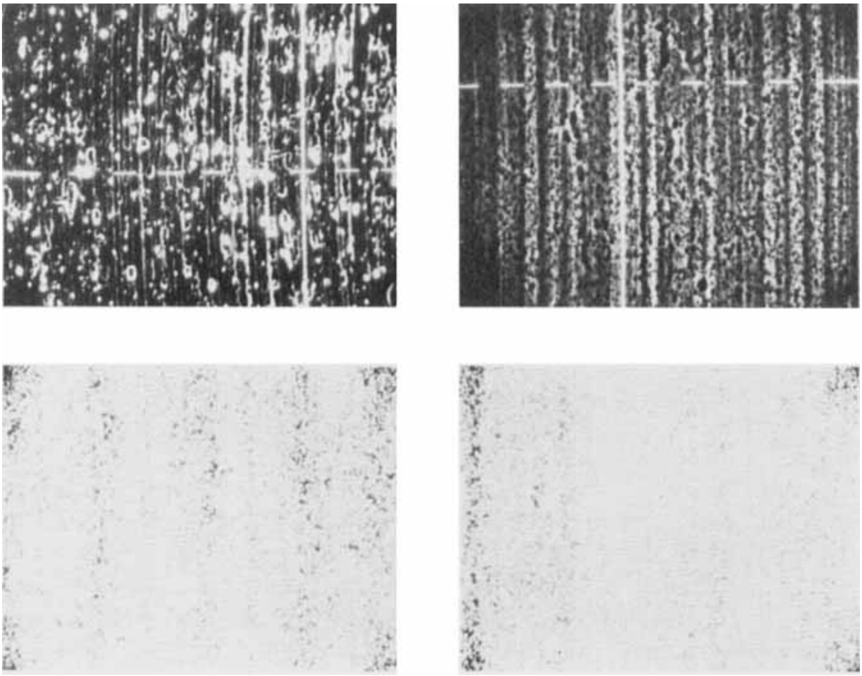

FIGURE 2 0.1% copper alloy, magnification 2000, sample A. Top, SEM of etched (left) and anodized (right) samples. Bottom, Al distributions of above samples.

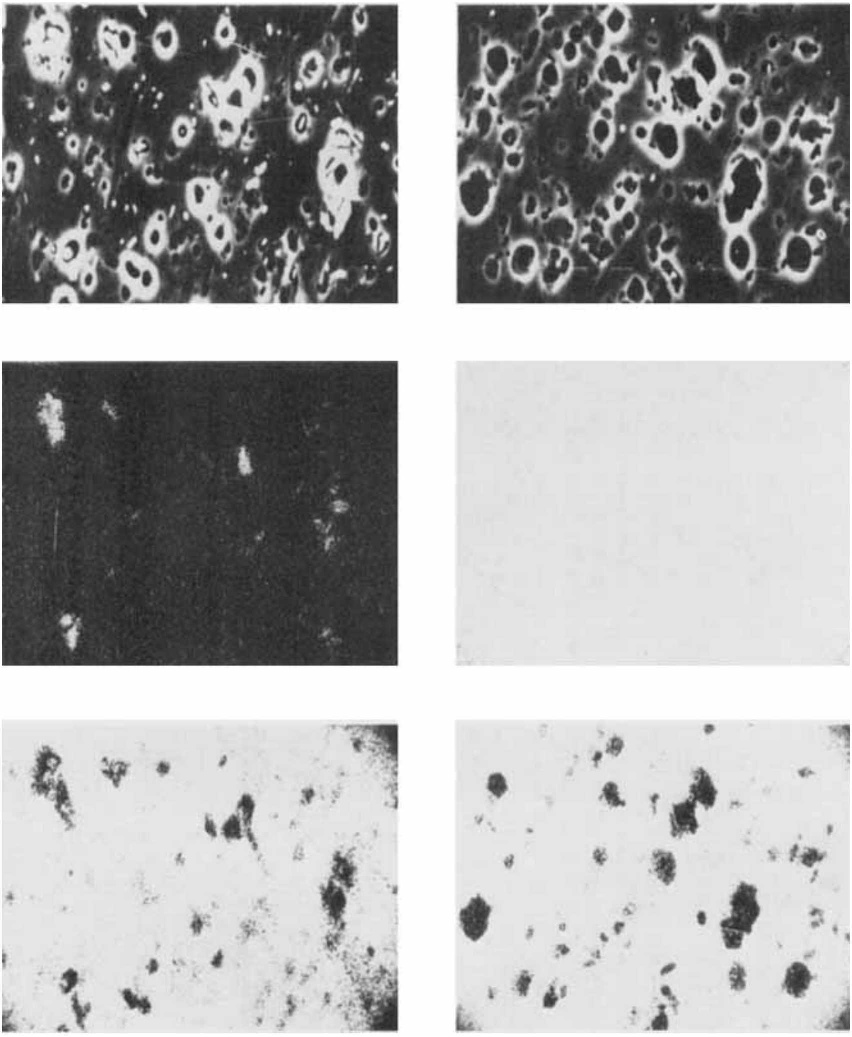

FIGURE 3 2.4% copper alloy, magnification 2000, sample B. Top, SEM of etched (left) and anodized (right) samples. Middle, Cu distributions of above samples. Bottom, Al distributions of above samples.

been produced during the etching process. The relatively much larger size of these pits completely masks the small pores (diameter ~ 320 Å) produced during anodization and consequently both the etched and anodized samples look very similar.

The X-ray emission analysis shows that in both cases the pits are more than

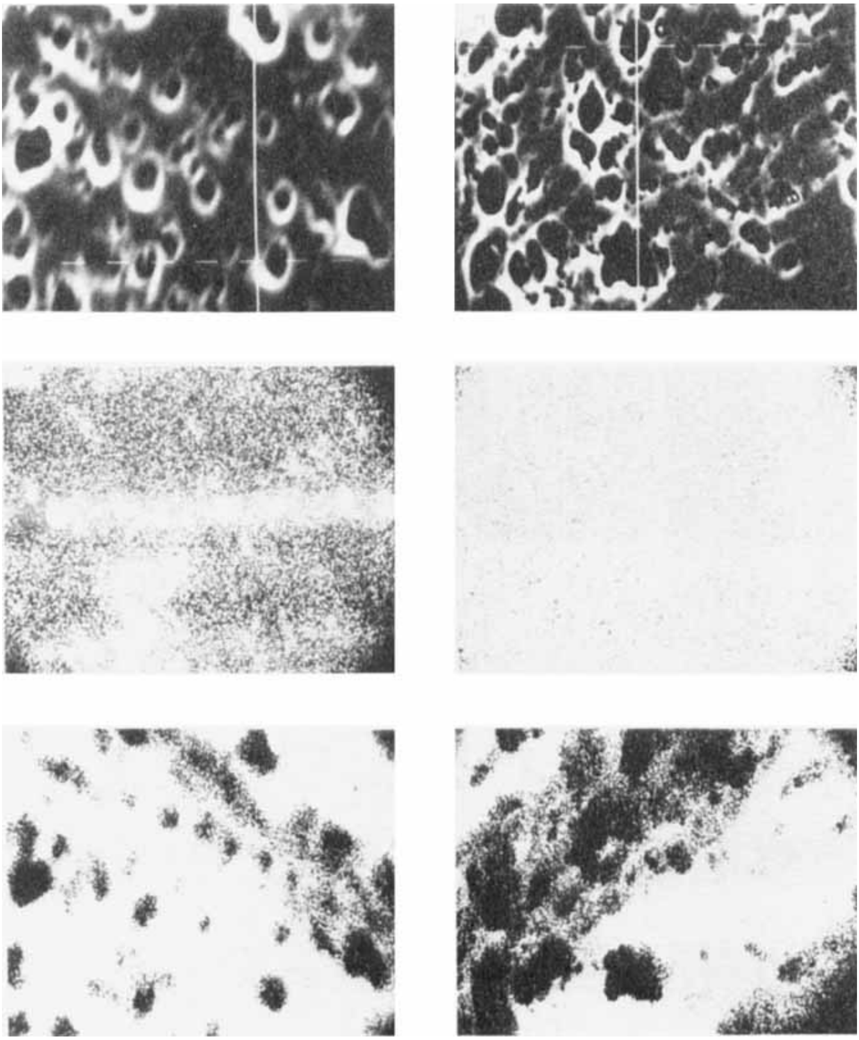

FIGURE 4 5.5% copper alloy, magnification 2000, sample C. Top, SEM of etched (left) and anodized (right) samples. Middle, Cu distributions of above samples. Bottom, Al distributions of above samples.

1 μm deep. This is evident from the micrographs showing the distribution of aluminium over the surface analysed by 25 KeV electrons. At the same time it is interesting to note that, after etching, the distribution of copper over the surface is quite uneven with an accummulation of copper in certain regions. After anodization the total number of holes remains the same though there is an increase in their size. However, the distribution of copper is now quite uniform.

Specimens of sample C show the general features of sample B but the effects are more pronounced. Once again the etched and anodized samples are characterized by large pits. In this case the pits are even larger than those found in sample B. On anodization the total number of pits remains approximately the same, but again their sizes are increased, some of the pits being as wide as 25 μm.

From the distribution of aluminium over the surface it is evident that the pits are deep (more than 1 μm). Also the etched sample shows an uneven distribution of copper, which bears no obvious relation to the pit structure, whereas the distribution after anodization appears uniform.

XPS signal profiles

The signal profiles of the components of the samples obtained during ion-etching are given in Figures 5–8. Generally the intensities of the signals

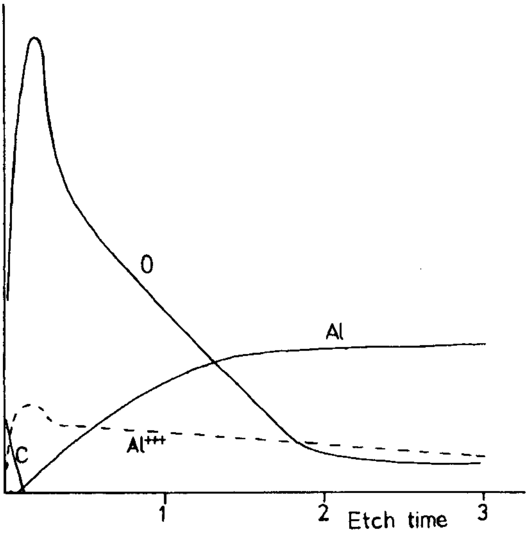

FIGURE 5 Depth profiles of etched 0.1% copper alloy, sample A (etch time units, μA m $\times 10^{-3}$).

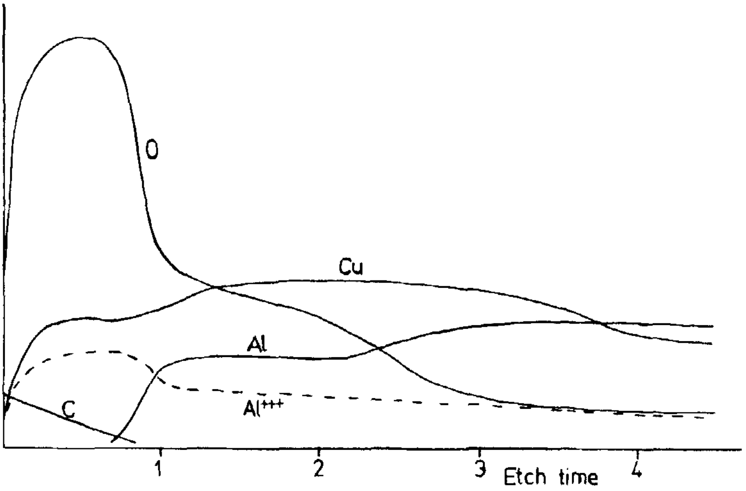

FIGURE 6 Depth profiles of etched 5.5% copper alloy, sample C (etch time units, μA m × 10^{-3}).

increase after a short ion bombardment as surface carbon contamination is removed. Additional carbon contamination penetrates the pore structures and is only removed gradually. In the case of the anodized sample, carbon is not negligible till the oxygen signal has decreased to the background value implying that the pores are completely filled by carbonaceous material.

The large difference in cross section for oxygen and aluminium results in the oxide film being more readily monitored by the Ols signal. Further the

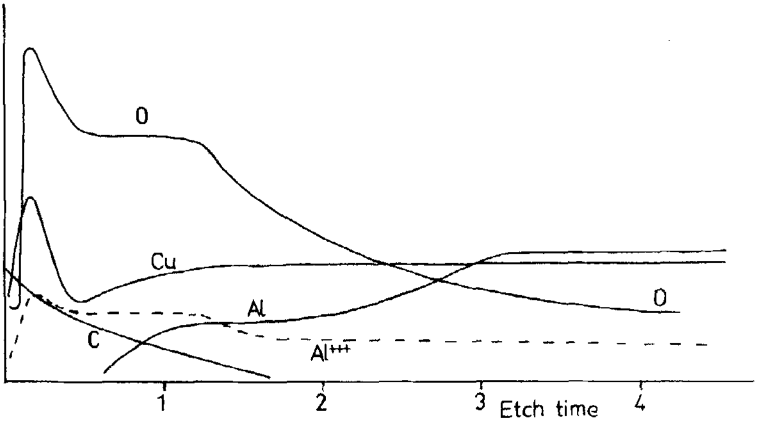

FIGURE 7 Depth profiles of etched 2.4% copper alloy, sample B (etch time units, μA m × 10^{-3}).

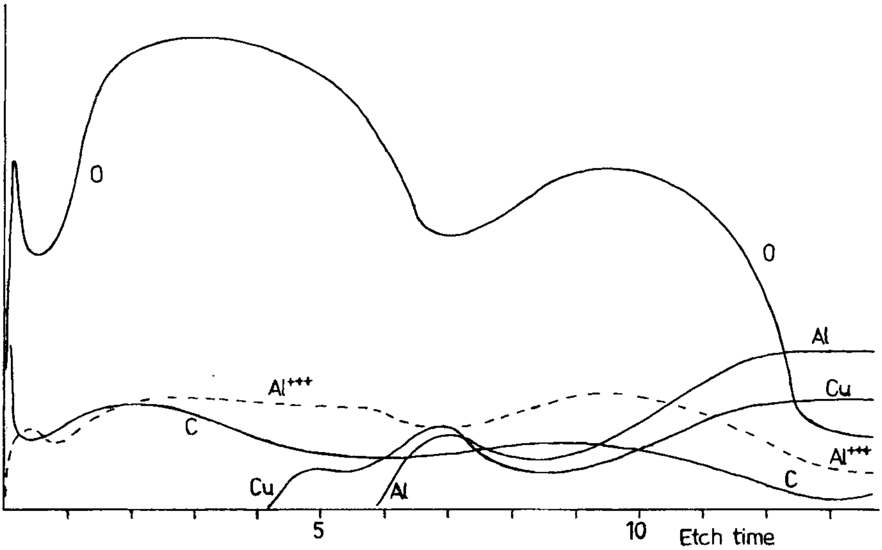

FIGURE 8 Depth profiles of anodised 2.4% copper alloy, sample B (etch time units, μA m × 10^{-3}).

oxidized aluminium peak is overlapped by the metallic aluminium peak which masks changes in the former.

The time required to remove the oxide film completely increases in the order A etched < B etched = C etched < B anodized. Anodization is known to increase the film thickness. The difference between the etched samples of A and the copper containing alloys will be discussed below.

Small amounts of chromium were detected in the early stages of ion etching of the etched samples.

DISCUSSION

It is obvious that the presence of copper has a marked effect on the surface morphology of aluminium alloys subjected to the processes of etching and anodization.

It is known for copper containing aluminium alloys that during the solution heat-treatment and subsequent quenching most of the copper is present in solid solution in the α phase.[12] The alloys are then hardened by the process of aging during which the copper precipitates out in the θ phase as $CuAl_2$. Since the exact thermal history and the extent of aging of commercial aluminium alloys is not known it can be assumed that the alloy consists of a mixture of copper in solid solution as well as in the form of $CuAl_2$. The aluminium solid solution separating out at the eutectic composition has 5.65% copper whereas the $CuAl_2$ intermetallic phase contains 52.5% copper. Examination of the micrographs showing the distribution of copper on the untreated specimens of samples B and C shows that the distribution is non uniform and that there are regions of very high copper. These should therefore correspond to the $CuAl_2$ intermetallic phase. It can also be seen that the density of these regions of high copper is higher in sample C than in sample B so that the amount of $CuAl_2$ in a particular sample appears to increase with the copper content of the sample. It has been suggested that regions of $CuAl_2$ in the alloy would be more susceptible to corrosion since the electrochemical potential of $CuAl_2$ is more cathodic than that of aluminium.[13] There are large holes in all the copper containing samples and the density and size of the pores is larger in the case of the samples having a higher copper content, which supports the above suggestion.

Depth analysis

Etched samples: aluminium and oxygen profiles Considering now the XPS data, the simplest results are given by the etched stub of sample A. The first appearance of aluminium metal indicates that the oxide has been removed from certain regions. The oxide is known to have a columnar structure with a thin coherent region at the metal interface. A step type oxygen depth profile may therefore be expected. The diffuse nature of the oxygen profile must then arise from the non-uniform nature of the surface. Though in this case there are few large pits, the surface shows a profusion of very small pores as has been noted in the literature. The true depth profile will only be obtained by convoluting the observed profile with a depth resolution function.

The etched stubs of samples B and C have even more diffuse oxygen signal profiles. The extensive formation of pits in these samples has been shown above. Ion etching is therefore removing material at all angles to the ion beam. It is necessary then to consider the nature of the ion etch process in more detail.

Sputtering rates are strongly matrix and angle of incidence dependent.[14] Elemental copper and aluminium have widely different sputter rates and these relative rates may change on alloying. The variation in sputtering rate with angle for many substances, including alumina, is known to take the form of an increase in rate, as the angle is decreased from the normal to the surface, to give a maximum rate, and then a decrease to a low value at small angles. The apparent thickness of an oxide film of constant real thickness will also vary with angle as the reciprocal of the sine of the angle. As the angle is decreased from the normal the increase in apparent thickness will be compensated to some extent by the increase in sputtering rate. The time taken to remove the oxide layer may therefore be approximately constant over this region. Further decrease in angle, beyond the point at which the maximum sputter rate occurs, will be in a region where the sputter rates and apparent thickness diverge rapidly. Therefore below a certain angle of incidence the time to remove the oxide layer will increase considerably. A further factor is that the electrons emitted during XPS analysis will not reach the analyser from surface regions corresponding to low angles of incidence of the ion beam, *i.e.* steep walls of pits or pores, because of shadowing. There will be a 'cut-off' point where above a certain apparent oxide thickness there will be no contribution to the oxygen signal. Two regions may therefore be expected in the oxygen depth profile. First a region where little or no metallic aluminium is found, corresponding to removal of oxide from a range of angles about the normal. The boundary of this region will be marked by a sudden increase in the metallic aluminium signal. There will then be a diffuse region with a corresponding slow increase in the metallic aluminium signal.

The oxygen profile of etched sample C shows a broad maximum after which the oxygen and oxidised aluminium signals decrease markedly and the metallic aluminium signal increases correspondingly. The increase in oxygen signal initially may be attributed to rearrangement of the mesopore structure under ion bombardment. A second region is evident where the oxygen signal decreases slowly and there is a corresponding increase in metallic aluminium. The data from this sample are therefore in agreement with the above model.

The concentration profiles for etched sample B are less readily interpreted. The appearance of metallic aluminium, indicating the removal of the oxide layer from the readily accessible regions, does not coincide with the marked decrease in oxygen and oxidized aluminium signals. A possible explanation is that in this case surface damage has resulted in exposure of fresh oxide surface so masking the expected decrease.

Copper profiles Copper is observed from the start of the depth analyses in both etched samples B and C. For the 5.5% Cu sample, the copper signal is broad and consists partly of oxidised and partly of metallic copper. The proportion of metallic copper increases to 100% near the point at which metallic aluminium is observed. The metallic copper profile bears no apparent relation to the metallic aluminium profile. This does not mean necessarily that copper is present as the pure element. The sensitivity of XPS for copper is much greater than for aluminium. A small amount of copper, *e.g.* 2%, in an α-phase aluminium alloy would therefore give a comparable signal to the aluminium. Small amounts of a $CuAl_2$ phase would give a readily measurable copper signal but a small aluminium one, which would be negligible when large amounts of the α-phase are also present. The copper signal therefore will show no apparent relation to the aluminium if it arises from metallic copper or small amounts of $CuAl_2$. In combination with the SEM data, the copper profiles indicate that a major part of the copper signal is associated with the pit regions and is elemental copper or $CuAl_2$.

These considerations apply also to etched sample B. The fraction of oxidized copper is greater initially in this case; 100% at the surface.

Anodised sample B Anodization thickens the oxide film. The effect on the above model would be to broaden the two regions of oxide removal. Examination of the oxygen profile of sample B shows two broad regions; at low ion etch times one with no evidence of metallic aluminium, and at high ion etch times one with various amounts of metallic aluminium. The boundary between the regions is marked by a decrease in the oxygen signal and the appearance of the metallic aluminium signal.

Copper is not detected till just before the boundary. The escape depth of the copper $2p$ electron is less than that of the aluminium $2p$, so the absence of metallic aluminium at this stage suggests that the copper signal is not from the α-phase alloy, but from the metallic copper, or $CuAl_2$ in the pits. No oxidised copper was detected and this may be related to the homogeneous distribution of copper laterally as noted by SEM.

Carbon is detected in appreciable quantities throughout the analysis showing that the pits are filled with contaminant. Part of the oxygen signal may be associated with this carbonaceous material. The maxima in the carbon signal suggest that at certain stages pit contents become newly exposed because of the angle of erosion or the particular pit shape. Variations in signals from the other components will also result from such effects.

In summary, oxidized aluminium-copper alloys are likely to have an etch pit structure covering an extensive part of the surface. Interpretation of the depth profiles obtained by ion etching should take this into account.

Adhesive bonded to these alloys will probably be partly in contact with copper. Moisture is known to affect such bonds adversely. Investigations of bond durability should therefore encompass the study of the chemical heterogeneity of the surface exposed to the adhesive.

References

1. C. Towler, R. A. Collins and G. Dearnaley, *J. Vacuum Sci. Technol.* **12,** 520 (1975).
2. T. S. Sun *et al., Appl. Surf. Sci.* **1,** 202 (1978).
3. P. Doig and J. W. Eddington, *Phil. Mag.* **28,** 961 (1973).
4. P. Doig and J. W. Eddington, *Br. Corrosion J.* **9,** 461 (1974).
5. A. Pattnaik and J. D. Meakin, *J. Appl. Polym. Sci., Appl. Polym. Symp.* **32,** 145 (1977).
6. T. S. Sun *et al., Appl. Surf. Sci.* **5,** 406 (1980).
7. A. J. Kinloch, H. E. Bishop and N. R. Smart, *J. Adhesion,* To be published (1982).
8. Ministry of Defence (UK), *Defence Standard 03-2/1, Method O,* 22 (1970).
9. G. S. Kabayashi and D. J. Donnelly, *Boeing Co. Rept.* No. DG—41517 (1974).
10. J. W. Diggle, T. C. Downie and C. W. Goulding, *Chem. Rev.* **69,** 365 (1969).

11. A. J. Kinloch, *J. Adhesion* **10,** 193 (1979).
12. D. S. Clark and W. R. Varney, *Physical Metallurgy for Engineers* (Van Nostrand, New York, 1962).
13. K. R. Horn, ed., *Aluminium* Vol I, (Am. Soc. Metals, Metals Park, Ohio, 1967).
14. M. Kaminsky, *Atomic and Ionic Impact Phenomena on Metal Surfaces* (Springer-Verlag, Berlin, 1965).